Arabian Journal for Science and Engineering
https://doi.org/10.1007/s13369-022-07367-3

RESEARCH ARTICLE-MECHANICAL ENGINEERING

Modeling and Solution of Reaction–Diffusion Equations by Using the Quadrature and Singular Convolution Methods

O. Ragb[1] · Mohamed Salah[1] · M. S. Matbuly[1] · H. Ersoy[2] · O. Civalek[3,4]

Received: 18 March 2022 / Accepted: 29 September 2022
© King Fahd University of Petroleum & Minerals 2022

Abstract
In the present work, polynomial, discrete singular convolution and sinc quadrature techniques are employed as the new techniques to derive accurate and efficient numerical solutions for the reaction–diffusion equations. Three models, Fitzhugh-Nagumo, Newell–Whitehead–Segel, and tumor growth models, were presented. The equations of three models are reduced to nonlinear ordinary differential equations by using different quadrature schemes. Then, Runge–Kutta fourth-order method is employed to solve nonlinear ordinary differential equations. In addition, the MATLAB program is used to solve these problems. Comparisons between the new methods and the existing ones are included, demonstrating the ease of implementation and efficiency. Also, the calculated results are supported by four various statistical errors. It is found that the rate of error reaches $\leq$ 10–6 in discrete singular convolution depending on regularized Shannon kernel which is better than others. Further, a parametric analysis is presented to discuss the influence of diffusion and reaction parameters on the solution.

Keywords Differential equations · Runge–Kutta · Numerical solution · Discrete singular convolution · Quadrature approach

1 Introduction

Reaction–diffusion problems are nonlinear partial differential equations that play a significant role in mathematical complex modeling such as medicine, chemistry, biology, and mechanics [1–3]. Fitzhugh-Nagumo (FN) equations are mathematical models that arise frequently in many applications like transportation of nerve pulsation, logistic population growth, nuclear reactor theory, and autocatalytic chemical reaction [4–11]. Newell–Whitehead–Segel (NWS) partial differential equation has been utilized like a computational model in various systems such as Faraday instability, chemical reaction, and Rayleigh–Benard convection [12–15]. Also, tumor growth (TG) model represents a reaction–diffusion equation that uses mathematical modeling to illustrate the growth, size, and expansion of tumors [16–18].

Recently, researchers have applied different techniques to obtain the exact and numerical solutions to these problems. Abbasbandy [5] used the homotopy technique to get the solution of the FN equation. Hariharan and Kannan [8] employed the wavelet technique for studying the FN equation. Van Gorder [9] presented a variational technique to acquire the exact solutions for Nagumo reaction–diffusion equations. Hazrat et al. [11] proposed Galerkin finite element technique for studying a generalized FN equation. Mahgoub and Sedeeg [12, 13] solved the NWS equation via Elzaki Adomian decomposition technique. Aasaraii [14] introduced a differential transform approach for studying NWS. Pue-On [15] used the Laplace Adomian decomposition approach to present an exact solution for NWS. For solving TG equations involving nonlinear interactions, the exact solution is difficult. So, computational techniques have been used to solve them. For the numerical methods of this problem, Chen et al. [19] and Feng [20] investigated the finite difference (FD) approach for generalized FN equation. Teodoro [21] implemented finite element and Newton techniques for studying the FN equation. Bhrawy [22] applied the Jacobi–Gauss collocation technique to solve the generalized FN

✉ O. Civalek
civalek@yahoo.com

1 Department of Engineering of Mathematics and Physics, Faculty of Engineering, Zagazig University, Zagazig, Egypt

2 Department of Mechanical Engineering, Division of Mechanics, Akdeniz University, Antalya, Turkey

3 Civil Engineering Department, Akdeniz University, Antalya, Turkey

4 Department of Medical Research, China Medical University Hospital, China Medical University, Taichung, Taiwan

Published online: 21 October 2022

equation. Soliman [23] used the variational iteration with Adomian decomposition approaches for examining FN equations. Zahra et al. [24] applied the Cubic B-Spline methods to solve a generalized NWS problem.

Ruiz-Ramírez and Macías-Díaz [25] solved NWS equation by using a non-standard symmetry-preserving scheme. Inan [26] introduced the solution of generalized FN equation by using Crank–Nicolson exponential FD approach. Hilal et al. [27] employed two various FD schemes to obtain the computational solutions for the NWS equation. Gupta et al. [28] developed the variational iteration technique for examining nonlinear NWS equations. Singh et al. [29] used an effective approach depending on Sumudu transform scheme and homotopy polynomials to get the numerical solution of a nonlinear fractional Drinfeld–Sokolov–Wilson equation. For the growth of human tumors, we solve a one-dimensional equation. Hossine et al. [30] analyzed the growth of human tumors by FD method. Darbyshire [31] applied parallel programming to estimate the computational accelerate, for avascular tumor growth. Lee et al. [32] utilized a crossbred numerical method to solve the avascular tumor growth model. Ali et al. [33] investigated the avascular tumor growth model by FD method.

It can be mentioned that some studies using mathematical techniques or simulations in different areas such as viral research and flow analyses have been performed. Rihan and Rahman [34] examined the interactions between a malignant tumor and the immune system of healthy effector cells under human immunodeficiency virus by employing ordinary and delay differential equations. Jaroudi et al. [35] studied a brain tumor growth model with reaction–diffusion equations and two three-dimensional different numerical simulations. Laib et al. [36] developed a numerical model for general form of a system of nonlinear Volterra delay integro-differential equations and applied this model to novel coronavirus (COVID-19) epidemic in China, Spain, and Italy. He and Meng [37] investigated the lump and interaction solutions of generalized (3 + 1)-dimensional nonlinear wave propagation for fluid dynamics. Li et al. [38] simulated the two-phase compressible displacement problems via nonlinear partial differential equations, characteristics method and mixed finite volume element. Lee and Lee [39] presented the least-squares finite element solution with an adaptive mesh approach for Giesekus viscoelastic flow problems.

A differential quadrature scheme has also been developed for solving different differential equations. Jiwari et al. [40] employed the polynomial differential quadrature method (PDQM) for studying the generalized FN equations with time-dependent coefficients in 1D size. Salah et al. [41–43] solved wave propagation, Fisher and FN equations by PDQM with Runge–Kutta fourth order (RK4), perturbation with PDQ block-marching technique and DQM with Implicit Euler.

The objective of the present study is to compute the numerical solution for three models of nonlinear reaction–diffusion equation by various quadrature approaches. Also, up to knowledge of the authors, sinc differential quadrature (SDQM) and discrete singular convolution differential quadrature (DSCDQM) are not examined for nonlinear reaction–diffusion analysis. So, Fitzhugh–Nagumo (FHN), Newell–Whitehead–Segel (NWS), and tumor growth (TG) models are presented to demonstrate the accuracy and efficiency of these methods. These different methods of DQ depending on different shape function are applied as the first methods for solving such problems. These methods are combined with Runge–Kutta fourth order (RK4) to solve nonlinear reaction diffusion equations. For each scheme MATLAB code is designed. Computed results are compared with exact and available ones in literature. In addition, The numerical results are supported by four various statistical errors such Absolute error, RMS, L_2 and L_∞ errors [27, 40]. The computed results are very agreement with the analytical solutions. Also, the obtained results show ease of implementation, efficiency, and applicability of different DQM. Moreover, a parametric analysis is presented to discuss the effect of parameters on the solution.

The rest of the paper is organized as follows. Section 2 gives the formulation for three models of nonlinear reaction–diffusion equation as Fitzhugh-Nagumo (FN), Newell–Whitehead–Segel (NWS), and tumor growth (TG) models. In Sect. 3, our main contributions include: four schemes based on differential quadrature are presented as polynomial differential quadrature (PDQ) technique, sinc differential quadrature (SDQM) [44–47], discrete singular convolution (DSC) based on delta Lagrange (DLK) and Regularized Shannon kernels (RSK) [48–57], and Runge–Kutta fourth order (RK4) [41–43]. Some numerical examples are presented and discussed in Sect. 4. The paper includes a conclusion in Sect. 5.

2 Materials and Methods

The general form for nonlinear reaction–diffusion equation can be described as [1–3]:

$$U_t(x,\ y,\ t) = D\ \nabla^2 U(x,\ y,\ t) + \mu\ f(U(x,\ y,\ t)),$$
$$0 \le t \le T, \quad a \le x \le b, \quad c \le y \le d \tag{1}$$

where D is the diffusion (D > 0) and μ is the reaction parameters. $U(x,\ y,\ t)$ is an unknown function depending on the variables x, y, and t. $f(U(x,\ y,\ t))$ is a nonlinear function.

The boundary conditions are determined as:

$$\begin{aligned} A_1\ U(0,\ y,\ t) + B_1 \left.\frac{\partial U}{\partial x}\right|_{(0,\ y,\ t)} &= F_1(y,\ t), \\ A_2\ U(a,\ y,\ t) + B_2 \left.\frac{\partial U}{\partial x}\right|_{(a,\ y,\ t)} &= F_2(y,\ t) \end{aligned} \tag{2}$$

$$\begin{aligned} A_3\ U(x,\ 0,\ t) + B_3 \left.\frac{\partial U}{\partial y}\right|_{(x,\ 0,\ t)} &= F_3(x,\ t), \\ A_4\ U(x,\ b,\ t) + B_4 \left.\frac{\partial U}{\partial y}\right|_{(x,\ b,\ t)} &= F_4(x,\ t) \end{aligned} \tag{3}$$

The initial condition is explained as:

$$U(x,\ y,\ 0) = \Phi(x,\ y) \tag{4}$$

where A_i , B_i , F_i, $(i = 1, 4)$, and $\Phi(x,\ y)$ are known functions.

In this article, it is concerned to illustrate the numerical attitude of three test examples such FN model, NWS model, and prediction of TG model. These examples can be explained as follows:

2.1 FN Model

FN is considered as a nonlinear parabolic partial differential equation along the x-direction. FN equation is determined as [11]:

$$\begin{aligned} U_t(x,\ t) = D\ \nabla^2 U(x,\ t) + \mu\ (U(x,\ t) - \lambda) \\ \times\ (1 - U(x,\ t))\, U(x,\ t) \end{aligned} \tag{5}$$

The boundary conditions are written as [11]:

$$\left.\frac{\partial U}{\partial x}\right|_{(0,\ t)} = \frac{1}{4\sqrt{2}} csch^2\left(\frac{-1}{2\sqrt{2}} + \frac{t}{4} + c\right), \tag{6}$$

$$\left.\frac{\partial U}{\partial x}\right|_{(1,\ t)} = \frac{1}{4\sqrt{2}} csch^2\left(\frac{1}{2\sqrt{2}} + \frac{t}{4} + c\right) \tag{7}$$

The initial condition is expressed as [11]:

$$U(x,\ 0) = \frac{1}{2}\left[1 - coth\left(\frac{x}{2\sqrt{2}} + c\right)\right], \tag{8}$$

The exact solution for FN equation is given as [11]:

$$\begin{aligned} U_{\text{exact}}(x,\ t) = \frac{1}{2}\left[1 - \coth\left(\frac{x}{2\sqrt{2}} + \frac{2\lambda - 1}{4} t + c\right)\right], \\ t > 0,\ 0 \le x \le 1 \end{aligned} \tag{9}$$

where λ and c are arbitrary constants.

2.2 NWS Model

NWS model is considered as the interaction of the influence of the diffusion expression with the nonlinear effect of the reaction expression. Then NWS equation is formed as [27]:

$$U_t(x,\ t) = D\ \nabla^2 U(x,\ t) + \mu\ (U(x,\ t) - U^4(x,\ t)) \tag{10}$$

The boundary conditions are written as [27]:

$$U(0,\ t) = \left[\frac{1}{2} + \frac{1}{2}\ \tanh\left(\frac{21\ t}{20}\right)\right]^{2/3}, \tag{11}$$

$$U(1,\ t) = \left[\frac{1}{2} + \frac{1}{2}\ \tanh\left(\frac{-3}{2\sqrt{10}}(1 - \frac{7t}{\sqrt{10}})\right)\right]^{2/3} \tag{12}$$

The initial condition is expressed as [27]:

$$U(x,\ 0) = (1 + e^{\frac{3x}{\sqrt{10}}})^{-2/3}, \tag{13}$$

The exact solution for the NWS equation is given as [27]:

$$\begin{aligned} U_{\text{exact}}(x,\ t) = \left[\frac{1}{2} + \frac{1}{2}\ \tanh\left(\frac{-3}{2\sqrt{10}}(x - \frac{7t}{\sqrt{10}})\right)\right]^{2/3}, \\ 0 < t < T,\ \ 0 \le x \le 1 \end{aligned} \tag{14}$$

2.3 Prediction of TG Model

Due to incessant changes in time, the number of cancer cells is complicated to evaluate where it may increase, relief in a calm state, or die. So, the TG is given by a nonlinear reaction–diffusion mathematical model as [30]:

$$U_t(x,\ t) = D\ \nabla^2 U(x,\ t) + \mu\ \rho\ U(x,\ t) \tag{15}$$

The boundary conditions are formed as [30]:

$$\left.\frac{\partial U}{\partial x}\right|_{(0,\ t)} = 0, \tag{16}$$

$$\left.\frac{\partial U}{\partial x}\right|_{(50,\ t)} = 0 \tag{17}$$

The initial condition is explained as [30]:

$$U(x,\ 0) = \frac{1}{\sqrt{2\pi}\ \varepsilon} e^{-\frac{1}{2}(\frac{x - x_0}{\varepsilon})^2}, \tag{18}$$

where ρ is the net proliferation rate $= 0.012\ \text{day}^{-1}$, $\varepsilon = 0.01$. x_0 is the initial position of the tumor.

$$D\left(\text{cm}^2/\text{day}\right) = \begin{cases} \text{Grey zone} = 0.0013 & 0 \le x \le 7.5 \\ \text{White zone} = 0.0065 & 7.5 \le x \le 42.5 \\ \text{Grey zone} = 0.0013 & 42.5 \le x \le 50 \end{cases} \tag{19}$$

3 Method of Solution

In this section, the four schemes based on differential quadrature and Runge–Kutta fourth order are explained as the numerical solutions for solving FN, NWS, and prediction of TG models.

DQM is defined as the unknown U and its derivatives are approximated as a weighted linear sum of grid values as follows [58]:

$$\left.\frac{\partial U}{\partial X}\right|_{(X_i,\ t)} = \sum_{k=1}^{M} A_{ik}^{x} U(X_k,\ t), \quad \left.\frac{\partial^2 U}{\partial x^2}\right|_{(x_i,\ t)} = \sum_{k=1}^{M} B_{ik}^{x} U(x_k,\ t), \tag{20}$$

where A_{ik}^{x} and B_{ik}^{x} are the 1st and 2nd weighting coefficients [58].

The weighting coefficients depend on the choice of shape function. Thus, it is different for each scheme. The weighting coefficients of 1st and 2nd derivatives are given as follows [58]:

3.1 Polynomial Differential Quadrature Method (PDQM)

The solution steps by PDQM are summarized as follows [58]:

1. Discretize the spatial area using Chebyshev-Gauss–Lobatto nodal points [58]:

$$X_i = \frac{a}{2}\left[1 - \cos\frac{(i-1)\pi}{M-1}\right], \quad i = 1, 2, \cdots, M, \quad 0 \le X \le a \tag{21}$$

where M is the number of nodal points.

2. The weighting coefficients of 1st and 2nd derivatives are obtained as [58]:

$$A_{ij}^{x} = \begin{cases} \dfrac{\prod_{k=1, k\neq i}^{M} (X_i - X_k)}{(X_i - X_j)\prod_{k=1, k\neq j}^{M} (X_j - X_k)} & i \neq j \\ -\sum_{j=1, j\neq i}^{M} A_{ij} & i = j \end{cases} B_{ij}^{x}$$

$$= \begin{cases} 2A_{ij}\left(A_{ii} - \frac{1}{X_i - X_j}\right), & i \neq j \\ -\sum_{j=1, j\neq i}^{M} B_{ij} & amp;\ i = j \end{cases} \tag{22}$$

3.2 Sinc Differential Quadrature Method (SDQM)

The solution steps by SDQM are summarized as follows [44–47]:

1. Discretize the spatial area using uniform nodal points.

$$U(X_i) = \sum_{j=-M}^{M} \frac{\sin[\pi(X_i - X_j)/h_X]}{\pi(X_i - X_j)/h_X} U(X_j), \quad (i = -M,\ M),\ h_X > 0 \tag{23}$$

2. The weighting coefficients A_{ij}^{x},B_{ij}^{x} are expressed by differentiating Eq. (23) as:

$$A_{ij}^{x} = \begin{cases} \frac{(-1)^{i-j}}{h_X(i-j)} & i \neq j \\ 0 & i = j \end{cases}, \quad B_{ij}^{x} = \begin{cases} \frac{-2(-1)^{i-j}}{h_X^2(i-j)^2} & i \neq j \\ \frac{-\pi^2}{3h_X^2} & i = j \end{cases} \tag{24}$$

where h_X is the grid size.

3.3 Discrete Singular Convolution Differential Quadrature Method (DSCDQM)

The solution steps by DSCDQM are outlined as follows [48–57]:

1. Discretize the spatial area using uniform nodal points.
2. Two kernels of DSC are employed in such a problem.

Table 1 Comparison between numerical solution by PDQM, SDQM and analytical solution of FHN equation at $\lambda = 1$, $c = \pi/4$, $t = 0.001$ and $x = 0$

Techniques		Exact [10]	PDQM			SDQM		
M	Errors		Obtained results	L_2	L_∞	Obtained results	L_2	L_∞
5		− 0.262267	− 0.2619589	1.012×10^{-4}	0.0003	− 0.261212929	1.055×10^{-4}	0.0011
7		− 0.262267	− 0.2635560	1.019×10^{-4}	0.0010	− 0.26313110	1.383×10^{-5}	0.0008
9		− 0.262267	− 0.2591486	1.049×10^{-4}	0.0035	− 0.261913419	1.054×10^{-5}	0.0004
11		− 0.262267	− 0.27070029	2.222×10^{-4}	0.0091	− 0.2621344	8.775×10^{-6}	0.0004
13		− 0.262267	− 0.24930787	4.364×10^{-4}	0.0220	− 0.2619099	6.723×10^{-6}	0.0003
15		− 0.262267	− 0.3023175	0.0011	0.0429	− 0.262287701	4.153×10^{-6}	0.0001
CPU time (Sec)		–	0.054051 at M = 5			0.030414 at M = 15		

Table 2 Comparison between the numerical results by DSCDQM-DLK, DSCDQM-RSK and exact ones of FHN equation at different bandwidth (2H + 1), regularization parameter β, and points M ($t = 0.001,\ x = 0,\ \lambda = -1$ and $c = \pi/4$)

Methods		2H + 1	DSCDQM-DLK	DSCDQM-RSK			
M	Bandwidth			$\beta = 2*h_X$	$\beta = 5*h_X$	$\beta = 10*h_X$	$\beta = 20*h_X$
5		3	− 0.262937016	− 0.263038	− 0.263038	− 0.263038	− 0.263035
		5	− 0.2613301626	− 0.263038	− 0.263038	− 0.263018	− 0.263018
		7	− 0.2613301626	− 0.263038	− 0.263038	− 0.263018	− 0.263018
7		3	− 0.2630286355	− 0.27003148	− 0.27003148	− 0.262910	− 0.262910
		5	− 0.2628404872	− 0.27003148	− 0.27003148	− 0.262910	− 0.262910
		7	− 0.2650798415	− 0.27003148	− 0.27003148	− 0.262910	− 0.262910
9		3	− 0.2630725518	− 0.2670721	− 0.26333395	− 0.262910	− 0.262910
		5	− 0.2628584219	− 0.26397237	− 0.262356	− 0.262910	− 0.262910
		7	− 0.2629812511	− 0.26603161	− 0.26374430	− 0.262910	− 0.262910
Analytic solution [10]			− 0.26293432793				

Table 3 The stability of numerical results by DSCDQM-DLK and DSCDQM-RSK for FHN equation when $\lambda = 1$, $c = \pi/4$ at $t = 0.001$

M	Errors	DSCDQM-DLK (2H + 1 = 3)			DSCDQM-RSK (2H + 1 = 3, β = 10*h_x)		
		RMS	L_2	L_∞	RMS	L_2	L_∞
5		4.2217×10^{-4}	2.129×10^{-4}	3.1721×10^{-4}	3.4243×10^{-5}	1.5399×10^{-5}	3.0799×10^{-5}
7		2.1830×10^{-4}	1.4522×10^{-4}	3.5512×10^{-4}	1.9870×10^{-5}	1.7523×10^{-5}	3.5917×10^{-5}
9		1.5540×10^{-4}	1.3412×10^{-4}	2.2010×10^{-4}	1.6550×10^{-5}	1.2412×10^{-5}	3.2070×10^{-5}
11		5.1257×10^{-5}	4.4234×10^{-5}	4.9240×10^{-4}	8.1157×10^{-6}	5.3834×10^{-6}	1.9251×10^{-6}
13		4.6173×10^{-5}	2.3776×10^{-5}	3.4194×10^{-5}	5.6157×10^{-6}	3.3746×10^{-6}	9.4394×10^{-6}
15		2.1459×10^{-5}	1.2049×10^{-5}	1.7183×10^{-5}	2.1839×10^{-6}	1.2083×10^{-6}	3.3583×10^{-6}
CPU time (Sec)		0.119610 at M = 9			0.101777 at M = 5		

Table 4 Comparison between Proposed schemes, exact solution and Galerkin finite element method of FHN equation when λ = 1, c = π/4 at time 0.05

Methods X	Exact [10]	GFEM [11]	PDQM	SDQM	DSCDQM-DLK	DSCDQM-RSK
− 1	− 0.6983159	− 0.6983	− 0.69831592	− 0.698264749	− 0.6982847490	− 0.698304747
− 0.80	− 0.55510405	− 0.5551	− 0.555104058	− 0.5550231375	− 0.5550231375	− 0.5551231376
− 0.60	− 0.4490276	− 0.4490	− 0.02798852	− 0.4042980167	− 0.3856286127	− 0.449092671
− 0.40	− 0.3680187	− 0.3680	− 0.35681593801	− 0.3597946412	− 0.3530137615	− 0.368022596
− 0.20	− 0.30469781	− 0.3047	− 0.28494984562	− 0.299567340	− 0.28728232500	− 0.304685747
0	− 0.25429702	− 0.2543	− 0.23100505386	− 0.2502856123	− 0.25159055494	− 0.254276291
0.20	− 0.21359802	− 0.2136	− 0.19260475766	− 0.2018867797	− 0.2171643740	− 0.2133583
0.40	− 0.1803492	− 0.1803	− 0.1749673401	− 0.1797451996	− 0.18396561120	− 0.1803713083
0.60	− 0.15292821	− 0.1529	0.2777387999	− 0.1465085384	− 0.1418553775	− 0.1529653527
0.80	− 0.13013609	− 0.1301	− 0.1301360293	− 0.1301222427	− 0.1301222421	− 0.1301222421
1	− 0.11106801	− 0.1110	− 0.1110680011	− 0.1110564320	− 0.1110564327	− 0.111056432

Table 5 RMS error and execution time by presented methods for FHN equation when λ = 1, c = π/4 and x = 0 at different times

Time	PDQM		SDQM		DSCDQM-DLK		DSCDQM-RSK	
	RMS error	Execution time	RMS error	Execution time	RMS error	Execution time	RMS error	Execution time
0.001	2.5467×10^{-4}	0.159334	2.8102×10^{-4}	0.159610	4.2217×10^{-4}	0.119610	3.4243×10^{-5}	0.131777
0.002	4.9064×10^{-4}	0.167334	5.3362×10^{-4}	0.149210	8.2269×10^{-4}	0.101610	6.8393×10^{-5}	0.118624
0.003	7.0936×10^{-4}	0.157534	7.6154×10^{-4}	0.161610	0.0012	0.142190	1.0245×10^{-4}	0.115443
0.004	9.1221×10^{-4}	0.158474	9.6799×10^{-4}	0.159410	0.0016	0.101275	1.3642×10^{-4}	0.115443
0.005	0.0011	0.157334	0.0011	0.159112	0.0012	0.109610	1.7030×10^{-4}	0.115443

The first shape function is Delta Lagrange Kernel (DLK) which is defined as:

$$U(X_i) = \sum_{j=-H}^{H} \frac{\prod_{k=-\mathrm{H}}^{\mathrm{H}} (X_i - X_k)}{(X_i - X_j) \prod_{j=-H,\, j\neq k}^{H} (X_j - X_k)} U(X_j),$$
$$(i = -H,\ H),\ \ H \geq 1 \tag{25}$$

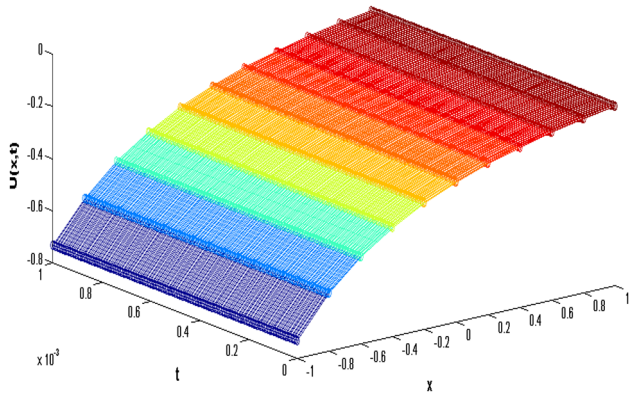
3. A_{ij}^x and B_{ij}^x are defined for DSCDQM-DLK as:

$$A_{ij}^x = \begin{cases} \frac{1}{(X_i - X_j)} \prod_{k=-H, k\neq i, j}^{H} \frac{(X_i - X_k)}{(X_j - X_k)} & i \neq j \\ - \sum_{j=-H,\, j\neq i}^{-H} A_{ij}^x & i = j \end{cases},$$

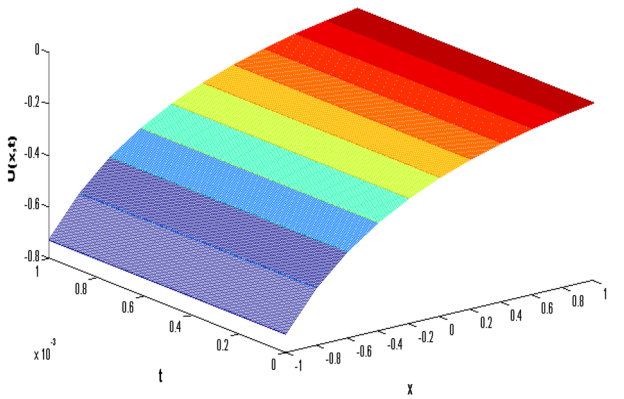
$$B_{ij}^x = \begin{cases} 2(A_{ij}^x . A_{ii}^x - \frac{A_{ij}^x}{(X_i - X_j)}) & i \neq j \\ - \sum_{j=-H,\, j\neq i}^{H} B_{ij}^x & i = j \end{cases} \tag{26}$$

(b) Second shape function is regularized Shannon Kernel (RSK) which is presented as follows:

$$U(X_i) = \sum_{j=-H}^{H} \left\langle \frac{\sin\left[\pi(X_i - X_j)/h_X\right]}{\pi(X_i - X_j)/h_X} e^{-\left(\frac{(X_i - X_j)^2}{2\beta^2}\right)} \right\rangle U(X_j),$$
$$(i = -M,\ M),\ \beta = (r * h_X) > 0 \tag{27}$$

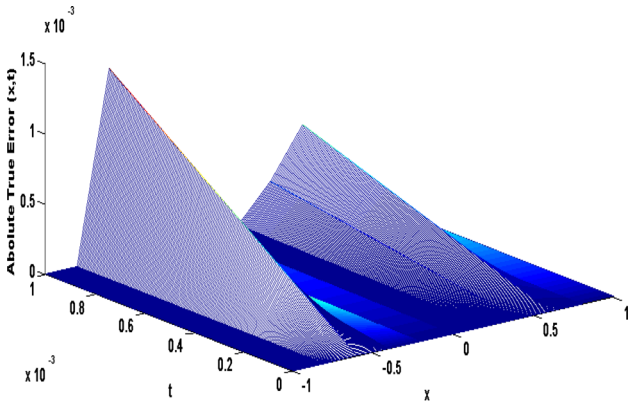


(a) Exact Solution

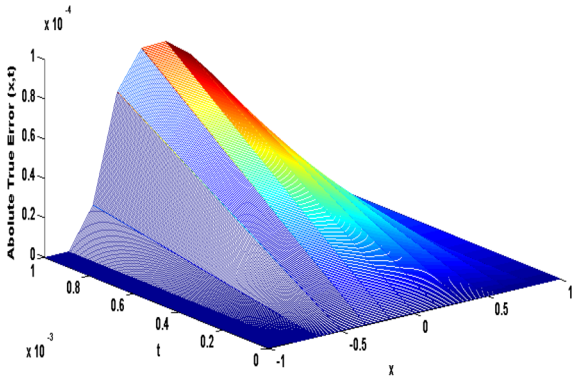


(b) DSCDQM-RSK

Fig. 1 Comparison between Exact solutions and DSCDQM-RSK in 3-D



(a) DSCDQM-DLK



(b) DSCDQM-RSK

Fig. 2 Absolute error at $\lambda = 1$ in 3-D for DSCDQM-DLK and DSCDQM-RSK

The weighting coefficients A_{ij}^{x},B_{ij}^{x} for DSCDQM-RSK are written as [48–57]:

$$A_{ij}^{x} = \begin{cases} \frac{(-1)^{i-j}}{h_X(i-j)} e^{-h_X^2\left(\frac{(i-j)^2}{2\beta^2}\right)}, & i \neq j \\ 0 & i = j \end{cases}, \; B_{ij}^{x}$$

$$= \begin{cases} \left(\frac{2(-1)^{i-j+1}}{h_X^2(i-j)^2} + \frac{1}{\beta^2}\right) e^{-h_X^2\left(\frac{(i-j)^2}{2\beta^2}\right)}, & i \neq j \\ -\frac{1}{\beta^2} - \frac{\pi^2}{3h_X^2} & i = j \end{cases} \tag{28}$$

where 2H + 1 is the effective computational bandwidth, β and r are the regularizations and computational parameters.

The problem is diminished to nonlinear ordinary differential equations by the substituting from Eq. (20) into Eq. (1) as follows:

$$\left.\frac{dU}{dt}\right|(x_i, y_j, t) = q_{ij}\left[U(x_1, y_1, t), U(x_2, y_1, t), \cdots, U(x_N, y_M, t)\right], \tag{29}$$

where

$$q_{ij} = D\left[\sum_{k=1}^{M} B_{ik}^{x} U(x_k, t) + \sum_{l=1}^{S} B_{jl}^{y} U(x_i, y_l, t)\right] + \eta f\left(U_{ij}\right), \quad i = (1, M), \quad j = (1, S). \tag{30}$$

3.4 Runge–Kutta Fourth Order (RK4)

To solve the nonlinear algebraic system in Eq. (30), RK4 is applied as follows [41–43]:

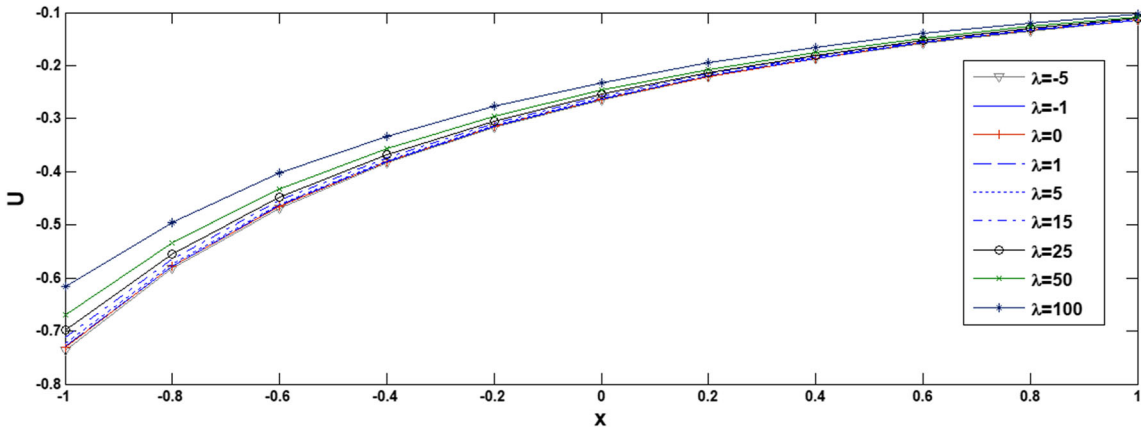


Fig. 3 The influence of λ on the results due to DSCDQM-RSK at t = 0.001

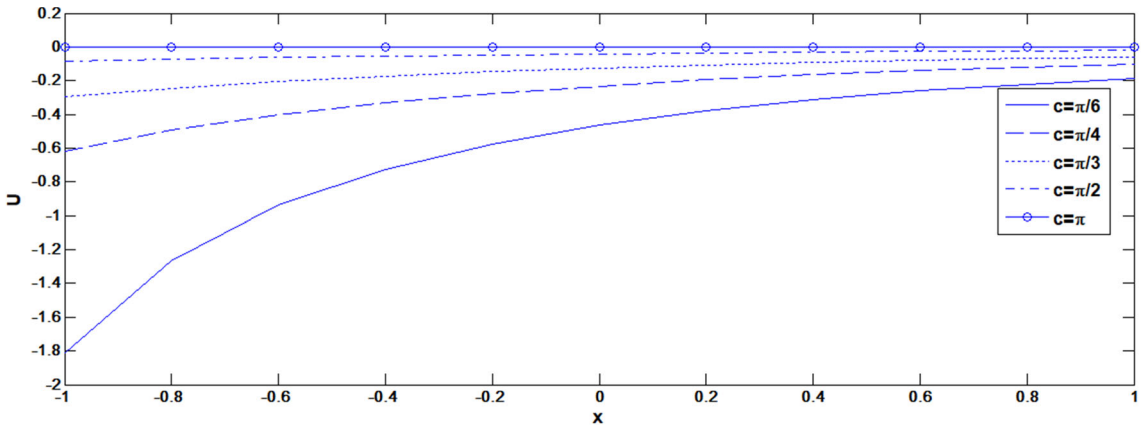


Fig. 4 The influence of c on the results due to DSCDQM-RSK at t = 0.001

Update the solution using RK4 such that [41–43]:

$$U(x_i, y_j, t_0 + \Delta t) = U(x_i, y_j, t_0) + \frac{1}{6}\left[K_1^{ij} + 2K_2^{ij} + 2K_3^{ij} + K_4^{ij}\right], \quad (31)$$

where

$$K_1^{ij} = \Delta t\, q_{ij}(U_{ij}, t_0), \quad (32)$$

$$K_2^{ij} = \Delta t\, q_{ij}\left(U_{ij} + \frac{K_1^{ij}}{2}, t_0 + \frac{\Delta t}{2}\right), \quad (33)$$

$$K_3^{ij} = \Delta t\, q_{ij}\left(U_{ij} + \frac{K_2^{ij}}{2}, t_0 + \frac{\Delta t}{2}\right), \quad (34)$$

$$K_4^{ij} = \Delta t\, q_{ij}(U_{ij} + K_3^{ij}, t_0 + \Delta t) \quad (35)$$

where t_0 is initial value of time,

Repeat Eq. (31) until the convergence of u reaches to its maximum or minimum for the given unstable (or stable) fold.

The condition of convergence is [41–43]:

$$\left|\frac{U_{k+1}}{U_k}\right| < 1 \qquad k = 0, 1, 2... \quad (36)$$

4 Numerical Results and Discussions

In this section, the nonlinear reaction–diffusion equations are solved by new techniques based on differential quadrature method and combined with RK4. To ensure the stability, reliability and accuracy of the numerical results, they were compared with the exact solution [10, 59] and numerical ones [11, 24, 27]. As well as, in numerical experiments various statistical errors are used to prove the convergence and stability of these techniques. Four statistical errors such as absolute error, RMS, L_2 and $L\infty$ errors are given by [27, 40]:

$$\text{Absolute Error} = |U_{numerical}(x_i, t_k) - U_{exact}(x_i, t_k)| \quad (37)$$

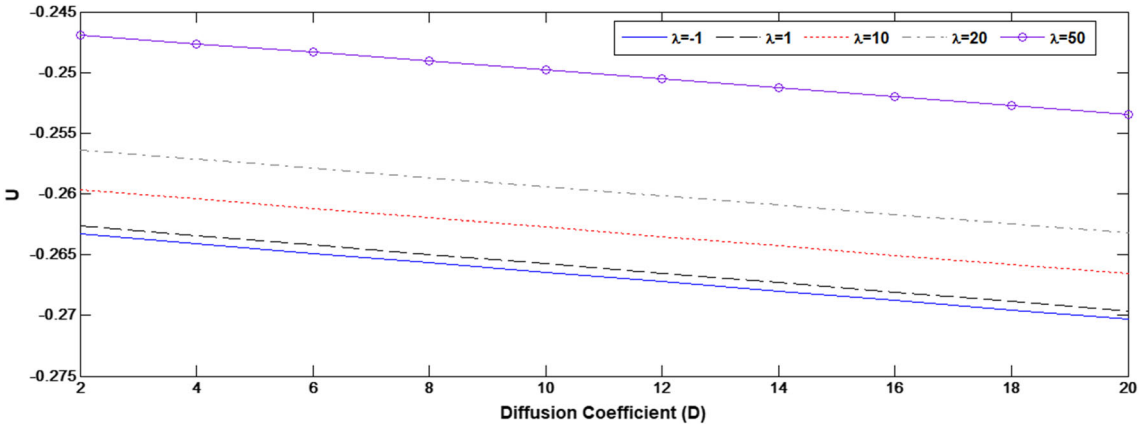


Fig. 5 The influence of D and λ on the results due to DSCDQM-RSK at $t = 1 \times 10^{-3}$, $x = 0$

Table 6 Comparison between the errors by PDQM, SDQM and other methods for NWS equation: $t = 0.1$

Techniques	PDQM (non-uniform)			SDQM		
M Errors	L_∞	RMS	Performance time (Sec)	L_∞	RMS	Performance time (Sec)
5	1.6480×10^{-5}	1.0144×10^{-5}	0.036524	4.2720×10^{-5}	2.5893×10^{-5}	0.028165
7	1.6782×10^{-5}	1.1508×10^{-5}	0.038157	8.8268×10^{-5}	4.6081×10^{-5}	0.030200
9	1.7561×10^{-5}	1.2225×10^{-5}	0.040702	1.5168×10^{-4}	6.9467×10^{-5}	0.031778
11	1.7908×10^{-5}	1.2657×10^{-5}	0.040750	2.3288×10^{-4}	9.5890×10^{-5}	0.034728
13	1.8057×10^{-5}	1.2941×10^{-5}	0.046016	3.3175×10^{-4}	1.2510×10^{-4}	0.036252
15	1.8212×10^{-5}	1.3158×10^{-5}	0.048226	4.4820×10^{-4}	1.5684×10^{-4}	0.037926

Table 7 Comparison between the RMS error by DSCDQM-DLK, DSCDQM-RSK and other techniques for NWS equation at different bandwidth (2H + 1), regularization parameter β, and points M: $t = 0.1$

Methods	2H + 1	RMS error $\times 10^{-4}$				
		DSCDQM-DLK	DSCDQM-RSK			
M bandwidth			$\beta = 2*h_X$	$\beta = 5*h_X$	$\beta = 7*h_X$	$\beta = 10*h_X$
5	3	738	6.9454	1.2971	0.71583	0.40308
	5	55	1.7074	0.53384	0.26144	0.17439
	7	9.3484	2.6057	1.1788	0.76279	0.54191
7	3	5.1949	7.9906	2.9939	1.5631	0.79332
	5	1.4563	3.6167	1.1542	0.55005	0.25233
	7	1.3389	12	2.5347	1.4122	0.78910
9	3	14	31	5.4985	2.8414	1.4119
	5	1.2666	16	1.9385	0.93673	0.43369
	7	1.1834	23	4.7267	2.5548	1.3375
CPU time (Sec)	0.033572 at M = 7, H = 2		0.031292 s at M = 5, H = 2			

Table 8 Absolute errors of the NWS model for proposed methods at different times and positions

Time	Methods	X	Absolute errors × 10^{-4}				
			0.2	0.4	0.6	0.8	1
0.2	UCBS [24]		3.800	8.190	11.12	11.84	10.80
	TCBS [24]		3.951	8.362	11.30	12.04	11.03
	ECBS [24]		9.673	19.00	24.46	25.19	22.51
	I-EFD [27]		0.366	0.346	0.278	0.208	0.149
	FI-EFD [27]		0.364	0.355	0.298	0.233	0.173
	PDQM (non-uniform)		0.9213	0.7630	0.6720	0.5013	0.35768
	PDQM (uniform)		1.548	1.486	1.220	0.9361	0.68678
	SDQM		1.546	1.486	1.220	0.9378	0.68678
	DSCDQM-DLK		1.546	1.486	1.220865	0.936108	0.68678
	DSCDQM-RSK		0.1237	0.1118	1.220865	0.877394	0.6370
0.4	UCBS [24]		4.230	11.11	16.13	17.77	16.58
	TCBS [24]		4.448	11.37	16.40	18.06	16.88
	ECBS [24]		11.59	26.41	35.87	38.05	34.62
	I-EFD [27]		0.352	0.367	0.304	0.231	0.166
	FI-EFD [27]		0.345	0.376	0.330	0.266	0.203
	PDQM (non-uniform)		1.432	1.499	1.266	0.9895	0.73381
	PDQM (uniform)		1.496	1.585	1.351	1.062	0.79402
	SDQM		1.492	1.585	1.351	1.062	0.79402
	DSCDQM-DLK		1.496	1.584	1.351	1.0623	0.79402
	DSCDQM-RSK		0.1195	0.1268	1.351	1.0623	0.7389797
0.6	UCBS [24]		2.890	10.08	15.69	17.89	17.03
	TCBS [24]		0.3111	10.34	15.96	18.18	17.34
	ECBS [24]		8.863e	24.44	35.12	38.38	35.58
	I-EFD [27]		0.365	0.392	0.335	0.262	0.194
	FI-EFD [27]		0.355	0.399	0.360	0.298	0.231
	PDQM (non-uniform)		1.5040	1.648	1.456	1.182	0.90684
	PDQM (uniform)		1.544	1.686	1.480	1.194	0.91127
	SDQM		1.541	1.6865	1.480	1.194	0.91127
	DSCDQM-DLK		1.541	1.68659	1.480	1.1942	0.91127
	DSCDQM-RSK		0.1123	0.1348	1.480	1.1942	0.91127

Table 9 L_∞ and L_2 errors of NWS model at $\Delta x = 0.05$ using DSCDQ RSK scheme, I-EFD [27] and FI-EFD [27]

Method	Δt	I-EFD [27]		FI-EFD [27]		DSCDQM-RSK	
	Time	L_∞ error × 10^{-6}	L_2 error × 10^{-6}	L_∞ error × 10^{-6}	L_2 error × 10^{-6}	L_∞ error × 10^{-8}	L_2 error × 10^{-8}
10^{-3}	0.01	313.1	126.0	312.9	125.4	11,184	4438.7
	0.1	413.4	295.4	410.1	288.6	14,372	10,004
	5	9.1	6.6	9.2	6.7	3.2818	2.1600
	10	0.0002511	0.0001830	0.0002529	0.0001843	0.00041229	0.00031411
10^{-4}	0.01	31.7	12.8	31.7	12.8	1060.5	428.95
	0.1	41.4	29.6	41.1	29.0	1379.7	992.27
	5	9.1	6.6	9.1	6.6	0.31695	0.21520
	10	0.0002495	0.0001815	0.0002497	0.0001817	0.00039772	0.00028529

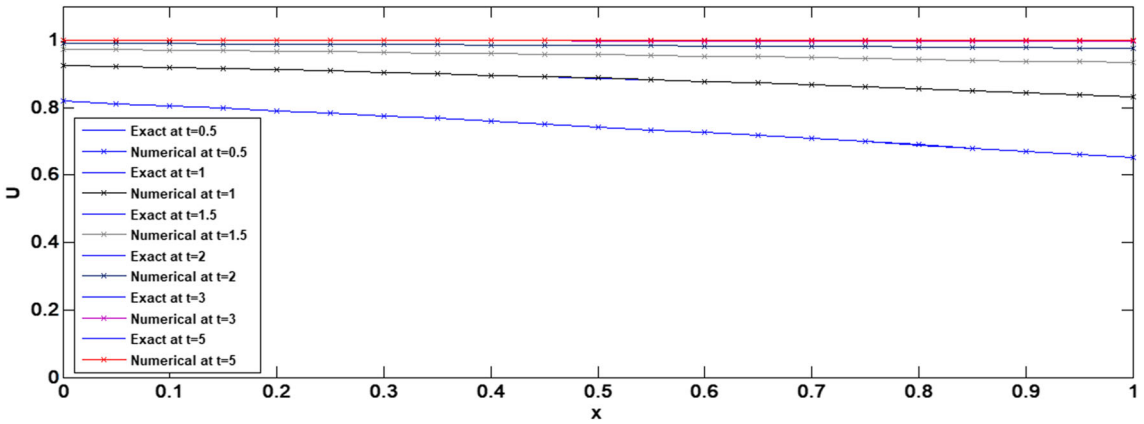


Fig. 6 Variation between DSCDQM-RSK solutions and Exact ones for NWS model at $\Delta t = 1 \times 10^{-3}$ and $\Delta x = 0.05$

$$\text{RMS Error} = \sqrt{\left[\sum_{i=1}^{M} (U_{numerical}(x_i, t_k) - U_{exact}(x_i, t_k))^2\right] \Big/ M} \tag{38}$$

$$L_2 \text{ Error} = \sqrt{\Delta x \sum_{i=1}^{M} (U_{numerical}(x_i, t_k) - U_{exact}(x_i, t_k))^2} \tag{39}$$

$$L_\infty \text{ Error} = \max_{1 \le i \le M} |U_{numerical}(x_i, t_k) - U_{exact}(x_i, t_k)| \tag{40}$$

Moreover, the efficiency of the proposed strategies is examined by computed CPU time under configuration (Intel(R)core (TM) i5-5200U CPU@2.20 GHz). All numerical computations have been done by designing the MATLAB program for each scheme.

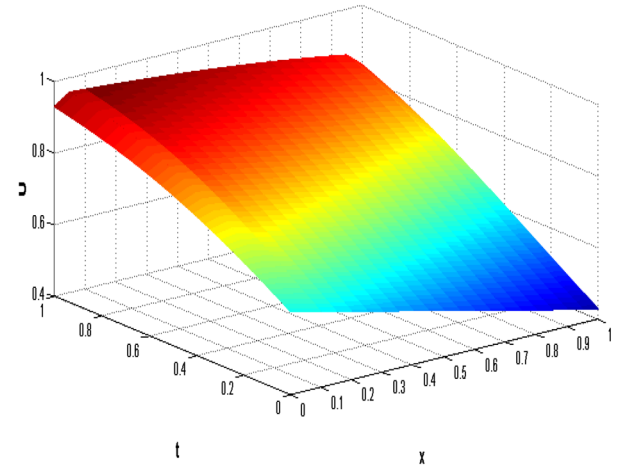
Three models are explained in detail as follow:

4.1 FN Model

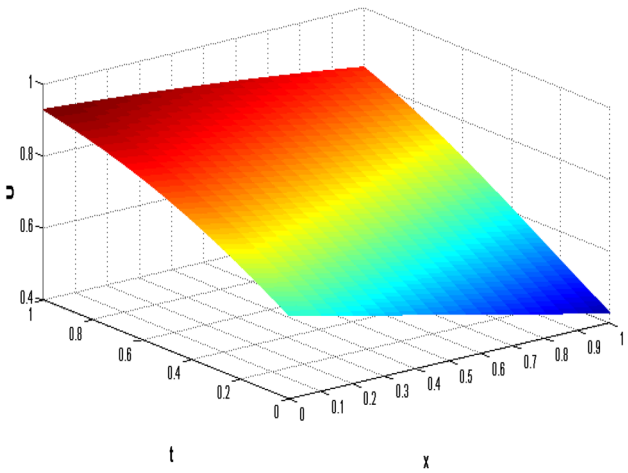
To validate the convergence, stability and efficiency of the solutions calculated by different techniques, the error measures are computed and compared with the exact [10] and numerical ones [11]. Numerical results obtained by four methods are presented as follow:

First, Table 1 shows the convergence between PDQM and SDQM. It is found that the computed results by SDQM are in good agreement with the exact ones at M = 15 and Classical DQM is unstable at a large number of nodes. Also, the values of errors $L_2 = 4.153 \times 10–6$, $L_\infty = 0.0001$ and CPU time = 0.030414 s for the SDQ technique are less than the PDQ technique. Thus, the SDQ scheme is accurate than the PDQ scheme.

Second, Tables 2 and 3 explain the stability of DSCDQM-DLK and DSCDQM-RSK. The obtained results from DSCDQM-DLK are converged at M = 7 and H = 2. While

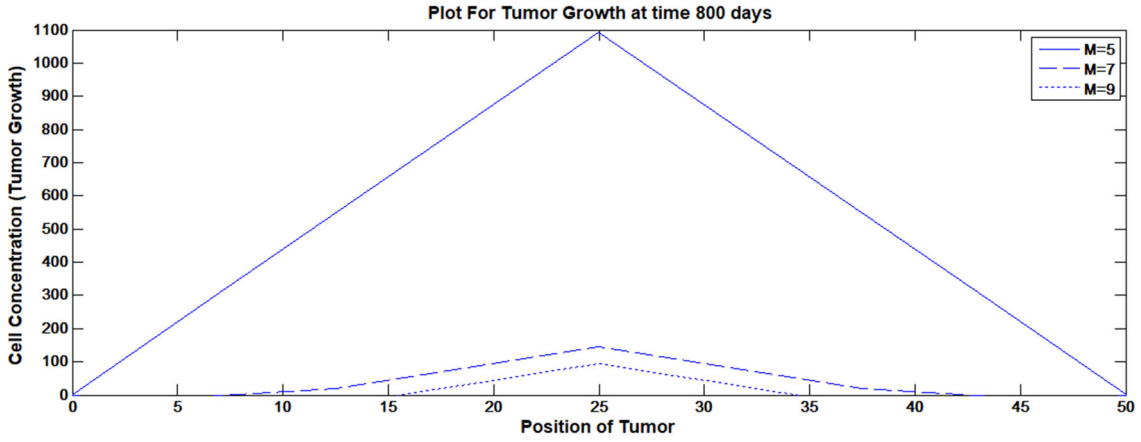


(a) DSCDQM-RSK

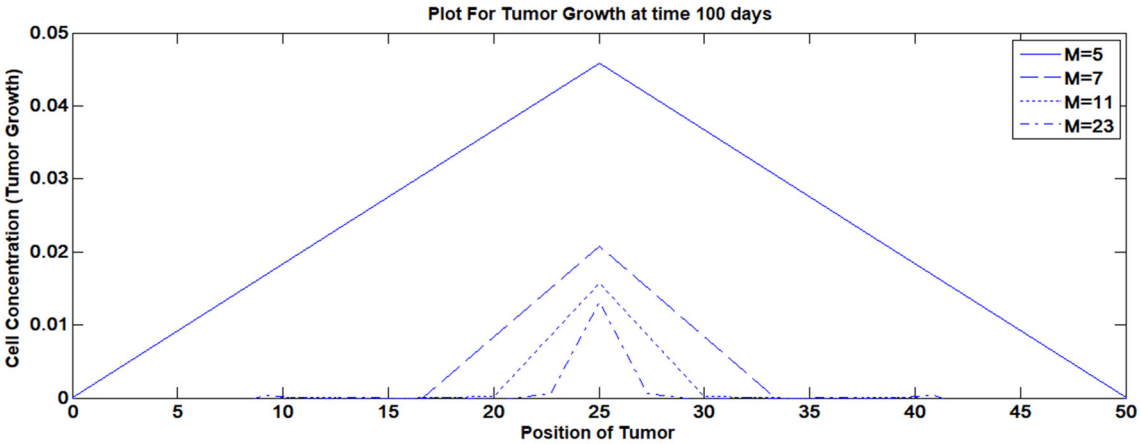


(b) Exact solutions

Fig. 7 Variation between DSCDQM-RSK solutions and Exact ones for NWS model in 3-D at $\Delta t = 0.05$ and $\Delta x = 0.1$



(a) PDQM non-uniform



(b) SINCDQM

Fig. 8 Comparison between PDQM and SDQM at different grid points and white region $x_0 = 25$

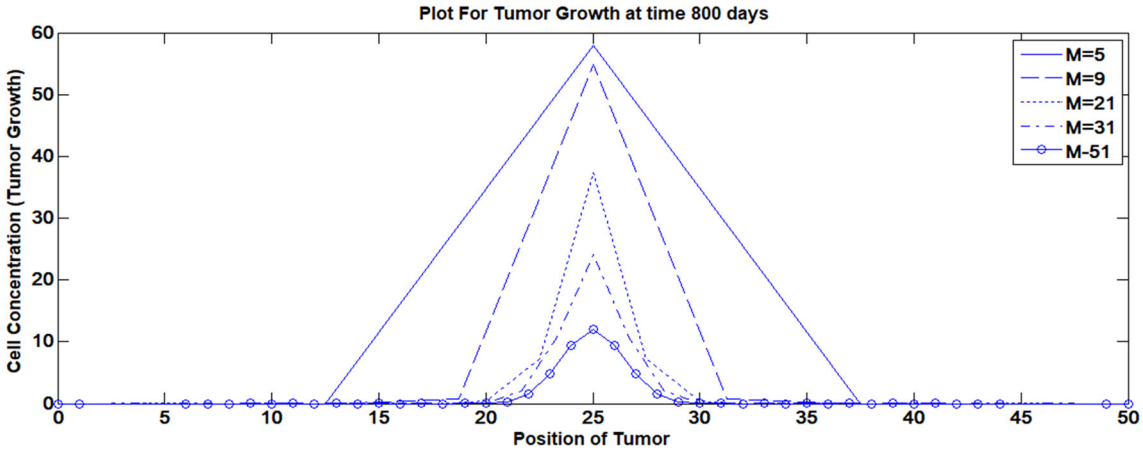
the solutions by DSCDQM-RSK are convergence at M = 5, H = 1 and β = 10*h_X. It is notice that the values of errors RSM = 3.4243 × 10–5, L_2 = 1.5399 × 10–5, L_∞ = 3.0799 × 10–5 and CPU time = 0.101777 for DSCDQM-RSK is less than the DSCDQM-DLK. Also, Table 4 displays the comparative study between the proposed methods, exact solution [10] and numerical results by Galerkin finite element method (GFEM) [11] at $-1 \leq x \leq 1$.

From the obtained results in tables (1–4), DSCDQM based on RSK at (2H + 1 = 3, β = 10*h_x) gives the accurate results better than Classical DQM, SDQM and DSCDQM-DLK at (2H + 1 = 3). As well as, the results by DSCDQM-RSK agree very well with the exact solution. Further, Table 5 verifies the accuracy of all present methods by calculating RMS error and execution time at different times ($0.001 \leq t \leq 0.005$). The best values of RMS = 3.4243 × 10–5 and CPU time = 0.131777 s at t = 0.001 are achieved by the DSCDQ-RSK scheme.

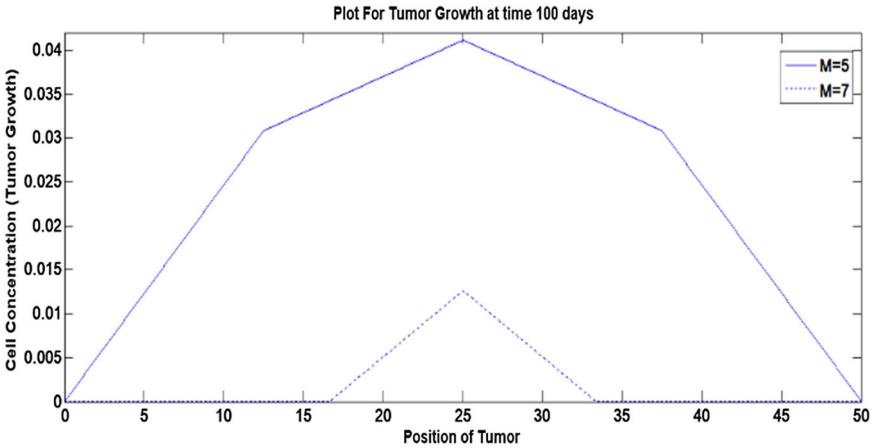
In addition, Fig. 1 shows the values of U(x,t) in 3D. Also, it shows DSCDQ-RSK scheme is very coinciding with the analytical solution. Figure 2 presents the calculation of absolute error of DSCDQM-DLK and DSCDQM-RSK. The value of absolute error is ≤ 10–4 for DSCDQ-RSK.

Finally, it is noted from Tables 1, 2, 3, 4 and 5 and Figs. 1 and 2 that DSCDQ-RSK is more stable, accurate, and efficient method than other ones. So, a parametric study based on DSCDQ-RSK are presented in Figs. 3, 4 and 5.

Figures 3, 4 and 5 show the influence of constant parameters λ, c and diffusion parameter D on the numerical results. The values of U(x,t) increase with the increase of λ, and it increases exponentially which its rate is very slow. But it decreases with the diffusion coefficients D increase. Then, the best value of λ at -1 ≤ λ ≤ 1 which the results converge. Also, the values of U(x,t) increase when increasing c and the results converges at c ≥ π/2.



(a) PDQM non-uniform



(b) SINCDQM

Fig. 9 Tumor growth using DSCDQM-DLK at different grid points and white region $x_0 = 25$

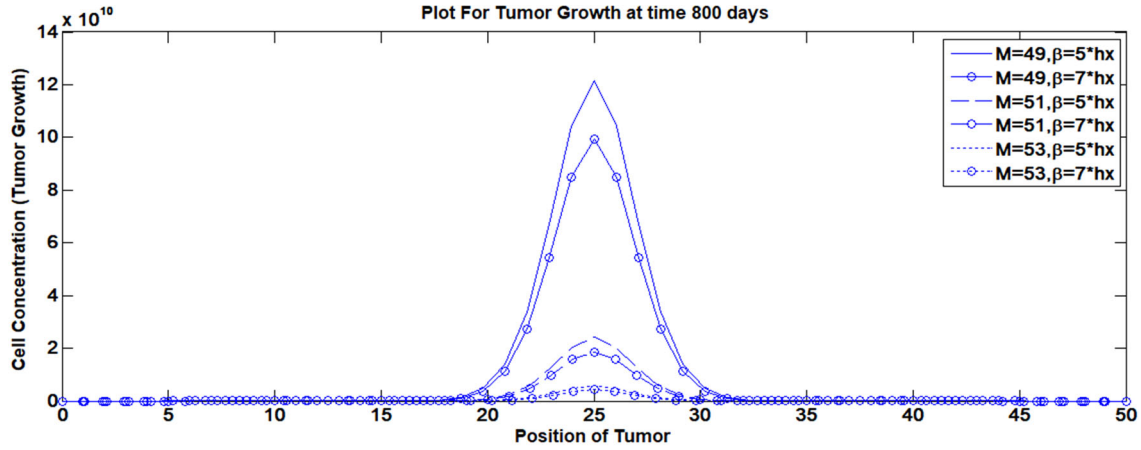
4.2 NWS Model

The accuracy stability and efficiency of the present techniques, the different error measures are calculated for the NWS equation and compared with other techniques [27]. Numerical results obtained by four methods are presented as follow:

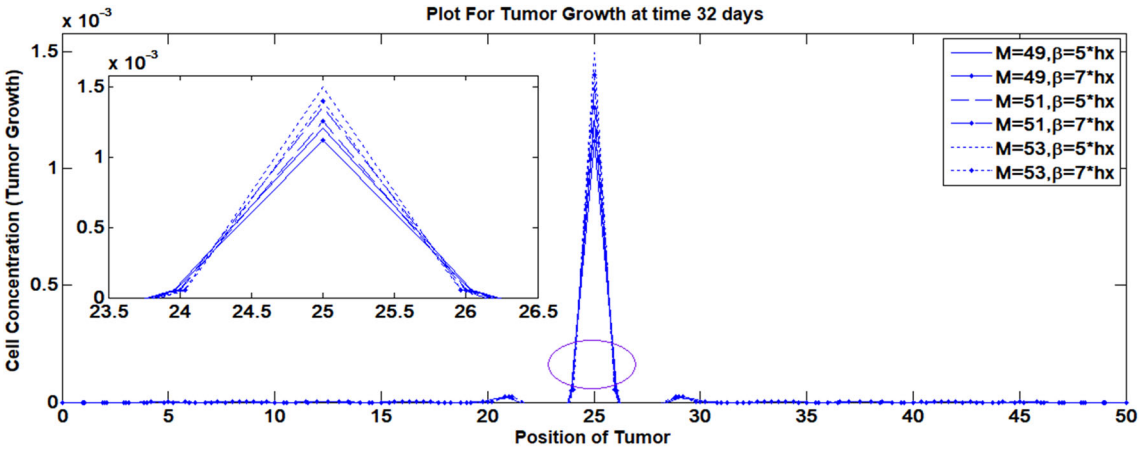
Firstly, Table 6 offers the stability and convergence of results between PDQM and SDQM. It is found that the calculated results by PDQM with Chebyshev discretization are more accurate than SDQM but CPU time in SDQM is less than PDQM. The least values of L_∞ error = 1.64 × 10–5, RMS = 1.014 × 10–5 for PDQM and CPU time = 0.028 s for SDQ technique.

Second, Table 7 introduces the stability of results between DSCDQ-DLK and DSCDQ-RSK schemes for the NWS equation. The obtained results from DSCDQM-DLK are converged at M = 7 and H = 2. While the results by DSCDQM-RSK convergences at M = 5, H = 2 and β = 10 *h_X.It is observed that the values of errors RMS = 1.7439 × 10–5 and CPU time = 0.031292 s for DSCDQM-RSK are lower than those for the DSCDQM-DLK. Table 8 presents the absolute errors of different quadrature schemes, and the previous methods used for solving the NWS equation [27] at T = 1, $\Delta t = 1 \times 10–3$ and x = 0.2:1. Table 9 offers L_∞ and L_2 errors of DSCDQ-RSK technique, implicit exponential FD approach (I-EFD) [27], Fully Implicit Exponential FD technique (FI-EFD) [27], Extended Cubic Uniform B-Spline (ECBS) [24], Trigonometric Cubic B-Spline (TCBS) [24], and Uniform Cubic B-Spline (UCBS) [24] for NWS equation at T = 10, $\Delta x = 0.05$ and 2 various options of Δt.

Figure 6 shows the exact and numerical results by the DSCDQ-RSK method for the NWS model at different times and positions, T = 5, $\Delta t = 1 \times 10–3$, $\Delta x = 0.05$. Also, Fig. 7 displays the analytical and computed results using the DSCDQ-RSK method in 3D. From these figures, it is



(a) H=1



(b) H=2

Fig. 10 Tumor growth using DSCDQM-RSK at different grid points and the white region at $x_0 = 25$

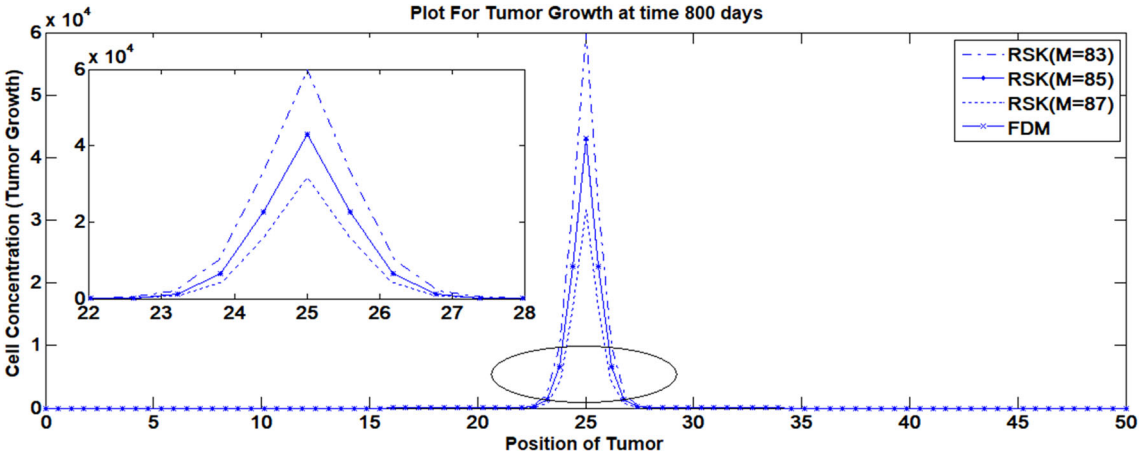
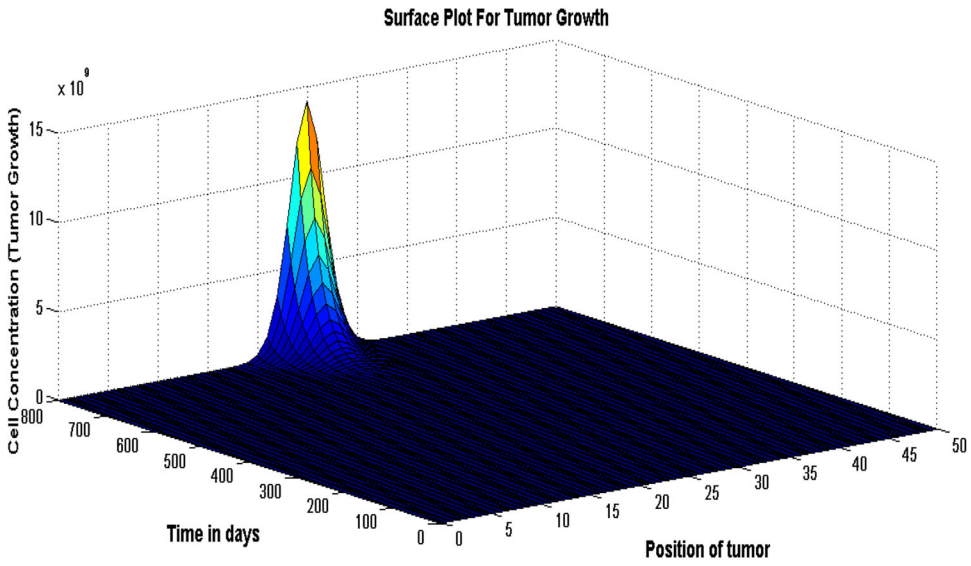
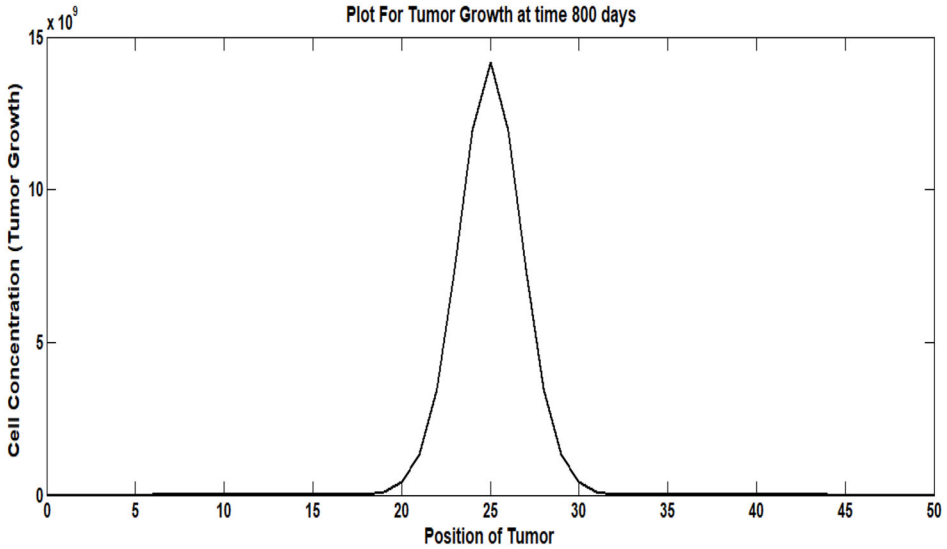


Fig. 11 Comparison between tumor growth using DSCDQM-RSK (H = 1, β = 24*hX) and FDM at different grid points and the white region at $\times\, 0 = 25$



(a) 3-D plot for Tumour Growth at each moment



(b) Tumour Growth at time t = T (800 days)

Fig. 12 Cell concentration of tumor growth at $x_0 = 25$ due to DSCDQM-RSK

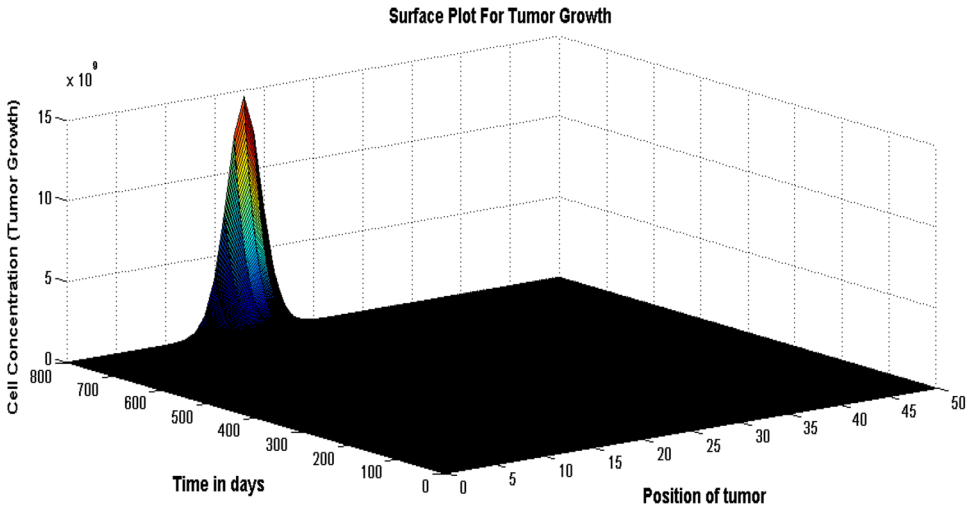
observed that the results of the DSCDQ-RSK technique agree very well with the analytical results [59].

Finally, from Tables 6, 7, 8 and 9) and Figs. 6 and 7, it is found that the DSCDQ-RSK scheme is more stable and convergent than other methods [24, 27, 59] at different times and positions.

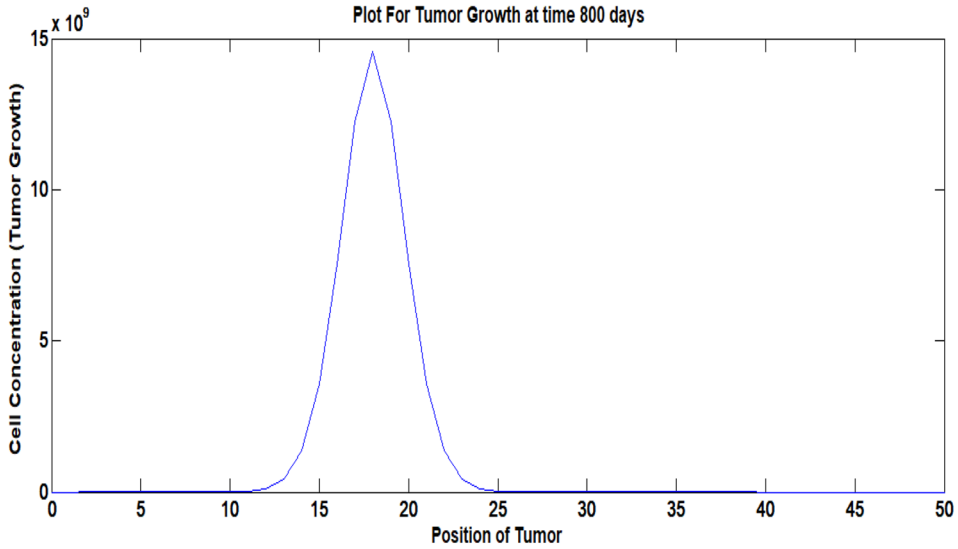
Furthermore, it must be mentioned that there are some problem in different applications for different length scale related to the model to enrich [60, 61] can be found in literature.

4.3 Prediction of TG Model

In such a problem, diffusion coefficient D is defined as a piece-wise function for various regions. The value of D in the white region equals to 5 D in the gray zone [30] however this may differ from patient to patient. Also, U(x,t) represents the tumor condensation of Glioma cells at time t and position x. The value of the Gaussian start profile for every region x_0 plays an important role in the prediction of growth [30]. So, the manner of the development of tumor condensation in terms of the speed of tumor cells for various values x_0 are studied by different quadrature techniques. The obtained results of tumor growth were changed due to variation of x_0



(a) 3-D plot for Tumour Growth at each moment



(b) Tumour Growth at time t = T (800 days)

Fig. 13 Cell concentration of tumor growth at $x_0 = 18$ due to DSCDQM-RSK

from grey region to white region as shown in Figs. 10, 11, 12, 13, 14, 15 and 16.

To verify the accuracy, convergence, and efficiency of the different quadrature results, the calculated solutions are compared with FDM [30].

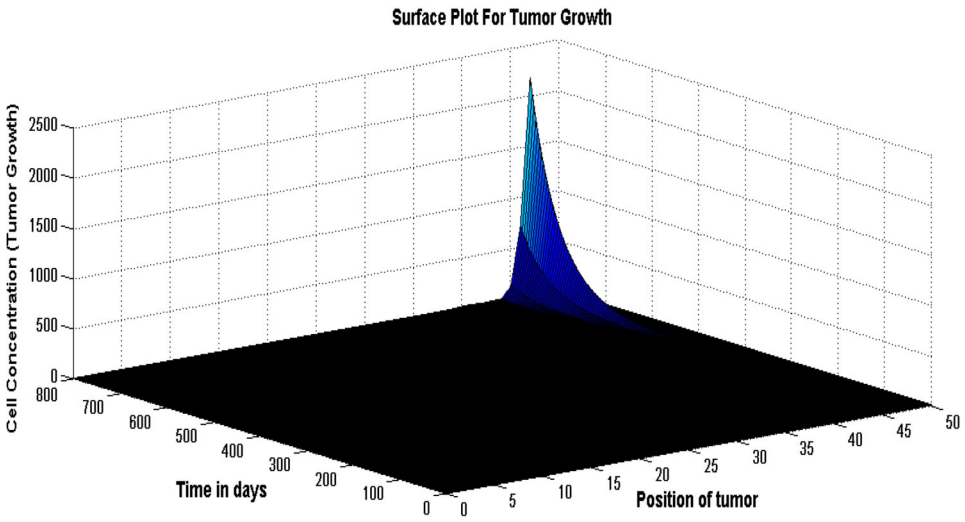
Numerical results obtained by four methods are presented as follow:

Firstly, Figs. 8, 9, 10 and 11 show the convergence of the proposed numerical methods. It is observed that the width of position tumor decreases and, tumor growth decreases with the increasing number of grid points (M). The maximum value for tumor growth is at $x_0 = 25$. The behavior of the graph is smooth curvy at a larger number of grid points. The regularization effect is investigated as shown in Fig. 10. Also, the regularization parameter (β) is inversely proportional to the cell concentration of the tumor.

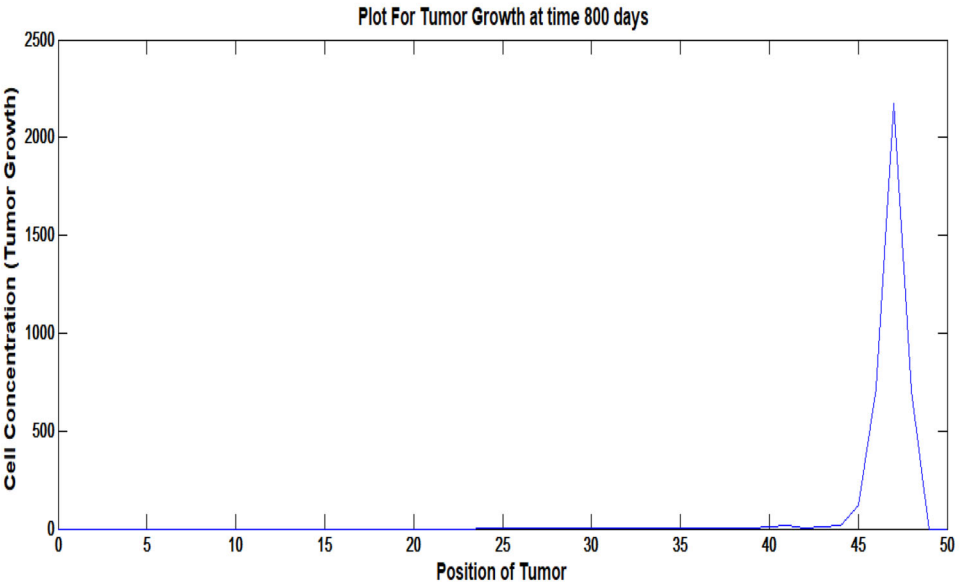
From these Figs. (8, 9, 10 and 11), it is observed that the calculated results by DSCDQM-RSK are compatible with FDM at M = 85, H = 1, $\beta = 24*h_X$ and CPU time = 0.406322 s.

Secondly, the results computed by other proposed techniques are unstable at a larger number of grid points (M). And therefore, the DSCDQ-RSK scheme is the best technique used for this problem.

Finally, Figs. 12, 13, 14, 15 and 16 explain the tumor growth prediction through 800 days and the maximum of growth that the tissue can carry at the different initial positions of the tumor ($x_0 = 25$, $x_0 = 3$, $x_0 = 18$, $x_0 = 47$, $x_0 = 30$ cm). Also, it is significant that the influence of x_0 is



(a) 3-D plot for Tumour Growth at each moment



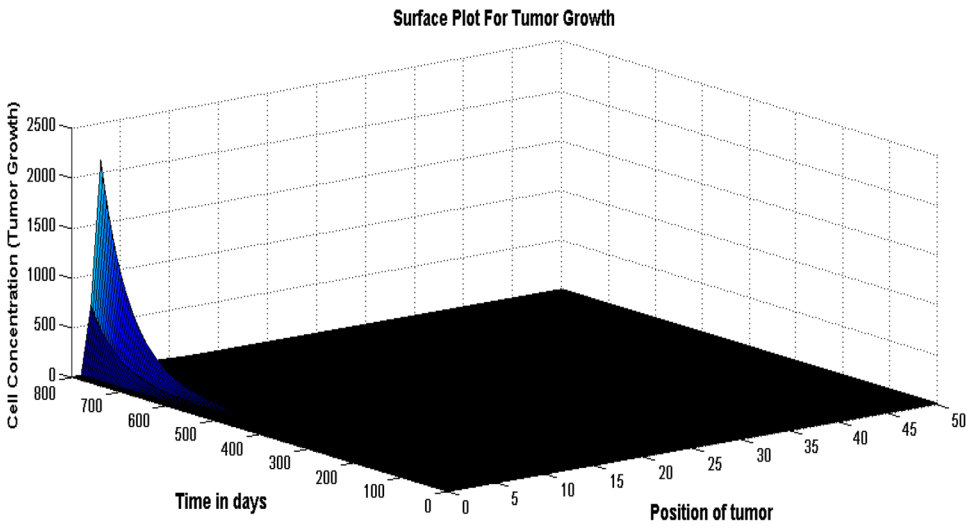
(b) Tumour Growth at time t = T (800 days)

Fig. 14 Cell concentration of tumor growth at $x_0 = 47$ due to DSCDQM-RSK

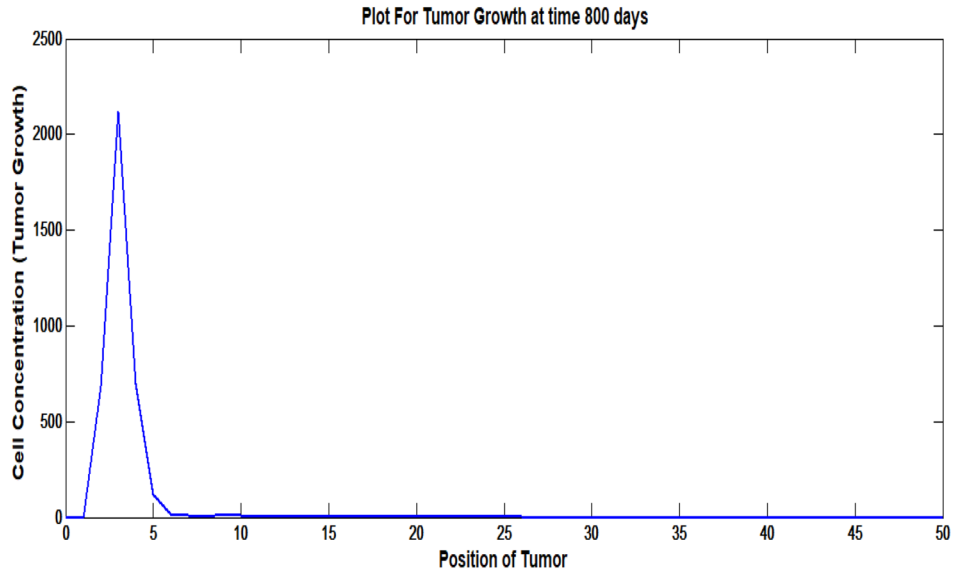
a very important role in predicting growth, which at $x_0 = 25$ the maximum of growth lies in zone 2, white region, and approximately reaches zero at x less than 20 or greater than 30. The cell concentration in the white region is larger than in the grey region. For zone 1, grey region, the maximum of growth is seen at x = 3 cm for $x_0 = 3$. As well as for zone 2, white region, the maximum of growth is seen at x = 18 cm for $x_0 = 18$. Also, for zone 3, grey region, the maximum of growth is seen at x = 47 cm for $x_0 = 47$. Further, for zone 2, white region, the maximum of growth is seen at x = 30 cm for $x_0 = 30$.

5 Conclusions

This paper investigates four strategies to solve three models of reaction–diffusion problems. Firstly, PDQM with uniform and Chebyshev discretization is utilized. After that, SDQM, DSCDQM-DLK, and DSCDQM-RSK are applied. Then, the problem is reduced to nonlinear ordinary differential equations. So, RK4 method is employed to complete the solution. A MATLAB code is designed for solving three test examples. These techniques are matched with the exact and other numerical results. In addition, a parametric analysis



(a) 3-D plot for Tumour Growth at each moment

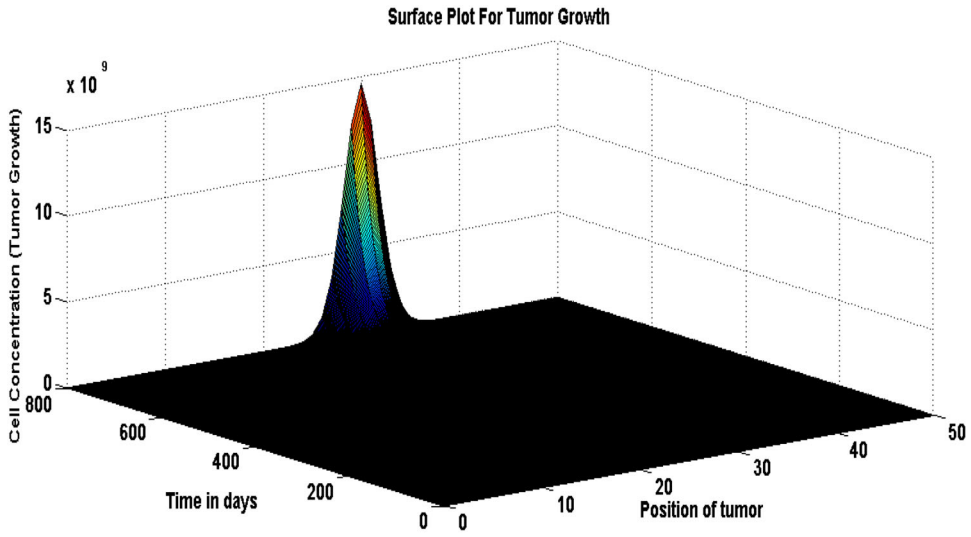


(b) Tumour Growth at time t = T (800 days)

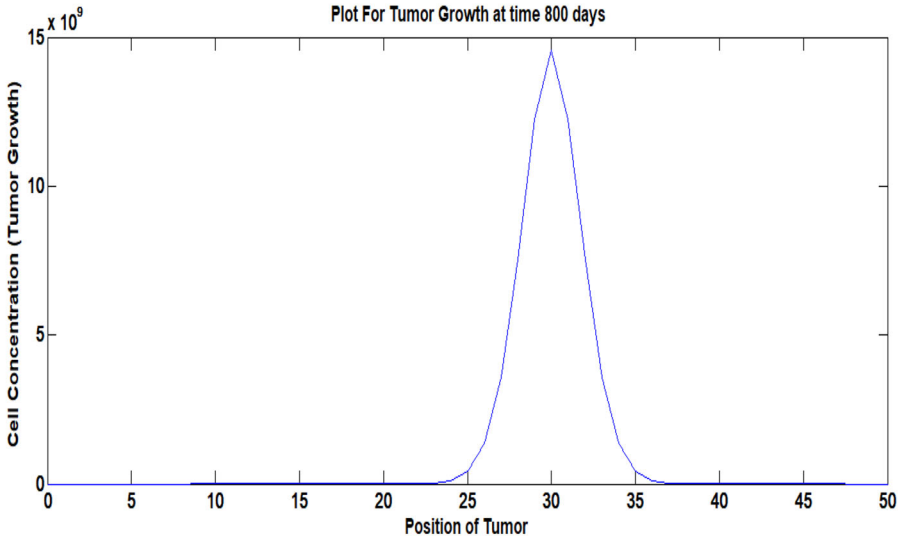
Fig. 15 Cell concentration of tumor growth at $x_0 = 3$ due to DSCDQM-RSK

is presented to examine the influence of diffusion and reaction parameters on the solutions. The most important points obtained from the results are:

- Numerical results by PDQM are unstable oscillatory results as much as grid steps > 11 and other strategies overcame the instability disadvantages arising with PDQM.
- DSCDQM-RSK is more stable, accurate, and efficient method to solve nonlinear reaction–diffusion equations than other techniques where:
- For FN equation the error reaches to ≤ 10–6, RMS ≤ 3.4243 × 10–5, L2 ≤ 1.53 × 10–5 and L∞ ≤ 3.07 × 10–5 at M = 5, H = 1, β = 10 *hx and CPU time = 0.101777 s.
- For NWS equation the error reaches to ≤ 10–6, RMS ≤ 1.7439 × 10–5 at M = 5, H = 2, β = 10 *hx and CPU time = 0.031292 s.
- For TG prediction equations the error reaches to ≤ 10–6 M = 85, H = 1, β = 24*hx and CPU time = 0.406322 s.
- Values of U (*x*,*t*) increase by increasing the value of λ and it decreases with the diffusion coefficients D increase.
- Values of U (*x*,*t*) increase when increasing *c*.
- It is noticed that the start location of a tumor is highly substantial to foretell the growth. And therefore, we can



(a) 3-D plot for Tumour Growth at each moment



(b) Tumour Growth at time t = T (800 days)

Fig. 16 Cell concentration of tumor growth at $x_0 = 30$ due to DSCDQM-RSK

foretell the growth of a tumor without any laboratory's exam.

Finally, we present methods that are applied for the first time for this type of problem and have proven their efficiency and accuracy compared to the existing results. These techniques can be applied to multivariant martensitic phase transformations between austenite and martensite and twinning between two martensite models [60]. We hope in the next research, we can use these methods to solve other types of complex problems.

Declarations

Conflicts of interest The authors certify that there is no conflict of interest with any individual/organization for the present work.

References

1. Mei, J.; Zhang, H.; Jiang, D.: New exact solutions for a reaction-diffusion equation and a quasi-Camassa holm equation. Appl. Math. E-Notes **4**, 85–91 (2004)
2. Fahmy, E.S.; Abdusalam, H.A.: Exact solutions for some reaction diffusion systems with nonlinear reaction polynomial terms. Appl. Math. Sci. **3**, 533–540 (2009)

3. Ropp, L.D.; Shadid, N.J.; Ober, C.C.: Studies of the accuracy of time integration methods for reaction–diffusion equations. J. Comput. Phys. **194**, 544–574 (2004)
4. Fitzhugh, R.: Impulse and physiological states in models of nerve membrane. Biophys. J. **1**, 445–466 (1961)
5. Abbasbandy, S.: Soliton solutions for the Fitzhugh-Nagumo equation with the homotopy analysis method. Appl. Math. Model. **32**, 2706–2714 (2008)
6. Hodgkin, A.L.; Huxley, A.F.: A quantitative description of membrane current and its application to conduction and excitation in nerve. J. Physiol. **117**, 500–544 (1952)
7. Abdusalam, H.: Analytic and approximate solutions for Nagumo telegraph reaction diffusion equation. Appl. Math. Comput. **157**, 515–522 (2004)
8. Hariharan, G.; Kannan, K.: Haar wavelet method for solving Fitzhugh-Nagumo equation. Int. J. Math. Stat. Sci. **2**, 59–63 (2010)
9. Van Gorder, R.A.: Gaussian waves in the Fitzhugh-Nagumo equation demonstrate one role of the auxiliary function H (x, t) in the homotopy analysis method. Commun. Nonlinear Sci. Numer. Simul. **17**, 1233–1240 (2012)
10. Li, H.; Guo, Y.: New exact solutions to the Fitzhugh-Nagumo equation. Appl. Math. Comput. **180**, 524–528 (2006)
11. Ali, M.; Kamrujjaman, M.M.; Islam, M.M.: Numerical computation of Fitzhugh-Nagumo equation: A novel Galerkin finite element approach. Int. J. Math. Res. **9**, 20–27 (2020)
12. Mahgoub, M.M.A.: Homotopy perturbation method for solving Newell–Whitehead–Segel equation. Adv. Theor. Appl. Math. **11**, 399–406 (2016)
13. Mahgoub, M.M.A.; Sedeeg, A.K.H.: On the solution of Newell–Whitehead–Segel equation. Am. J. Math. Comput. Model. **1**, 21–24 (2016)
14. Aasaraai, A.: Analytic solution for Newell–Whitehead–Segel equation by differential transform method. Middle East J. Sci. Res. **10**, 270–273 (2011)
15. Pue-on, P.: Laplace Adomian decomposition method for solving Newell–Whitehead–Segel equation. Appl. Math. Sci. **7**, 6593–6600 (2013)
16. Enderling, H.; Chaplain, M.A.: Mathematical modeling of tumor growth and treatment. Curr. Pharm. Des. **20**, 4934–4940 (2014)
17. Swanson, K.R.: Mathematical modeling of the growth and control of tumors. Ph.D. Thesis, University of Washington, Washington (1999)
18. Swanson, K.R.; Harpold, H.L.P.; Peacock, D.L.; Rockne, R.; Pennington, C.; Kilbride, L.; Grant, R.; Wardlaw, J.M.; Alvord, E.C.: Velocity of radial expansion of contrast-enhancing gliomas and the effectiveness of radiotherapy in individual patients: A proof of principle. Clin. Oncol. **20**, 301–308 (2008)
19. Chen, Z.; Gumel, A.; Mickens, R.: Nonstandard discretizations of the generalized Nagumo reaction-diffusion equation. Numer. Meth. Partial Differ. Equ. **19**, 363–379 (2003)
20. Feng, H.; Lin, R.A.: A finite difference method for the Fitzhugh-Nagumo equations. Dyn. Contin. Discrete Impuls Syst. Series B Appl. Algorithms **22**, 401–412 (2015)
21. Teodoro, M.: Numerical approximation of a nonlinear delay-advance functional differential equation by a finite element method. In: Simos, T.E.; Psihoyios, G.; Tsitouras, C. Anastassi Z. (eds) International Conference of Numerical Analysis and Applied Mathematics, pp. 806–809. Kos, Greece, **1479**, (2012)
22. Bhrawy, A.: A Jacobi–Gauss–Lobatto collocation method for solving generalized Fitzhugh-Nagumo equation with time-dependent coefficients. Appl. Math. Comput. **222**, 255–264 (2013)
23. Soliman, A.A.: Numerical simulation of the Fitzhugh-Nagumo equations. Abstr. Appl. Anal. 762516 (2012)
24. Zahra, W.K.; Ouf, W.A.; El-Azab, M.S.: Cubic B-spline collocation algorithm for the numerical solution of Newell- Whitehead-Segel type equations. Electron. J. Math. Anal. Appl. **2**, 81–100 (2014)
25. Macias-Dia, J.E.; Ruiz-Ramirez, J.: A non-standard symmetry-preserving method to compute bounded solutions of a generalized Newell–Whitehead–Segel equation. Appl. Numer. Math. **61**, 630–640 (2011)
26. Inan, B.: A finite difference method for solving generalized Fitzhugh–Nagumo equation. In: Tosun, M.; Ersoy, S.; Ilarslan K. (Eds) 6th International Eurasian Conference on Mathematical Sciences and Applications, Budapest, Hungary, 1926, 020018 (2018)
27. Hilal, N.; Injrou, S.; Karroum, R.: Exponential finite difference methods for solving Newell–Whitehead–Segel equation. Arab. J. Math. **9**, 367–379 (2020)
28. Gupta, S.M.; Goyal, M.; Prakash, A.: Numerical treatment of newell-whitehead-segel equation. TWMS J. App. Eng. Math. **10**, 312–320 (2020)
29. Singh, J.; Kumar, D.; Baleanu, D.; Rathore, S.: An efficient numerical algorithm for the fractional Drinfeld-Sokolov-Wilson equation. Appl. Math. Comput. **335**, 12–24 (2019)
30. Hossine, Z.; Meghla, A.; Kamrujjaman, M.: A Short review and the prediction of tumor growth based on numerical analysis. Adv. Res. **19**, 1–10 (2019)
31. Darbyshire, P.M.: A System of soupled nonlinear partial differential equations describing avascular tumor growth are solved numerically using parallel programming to assess computational speedup. Comput. Biol. Bioinform. **3**, 65–73 (2015)
32. Lee, H.G.; Kim, Y.; Kim, J.: Mathematical model and its fast numerical method for the tumor growth. Mathem. Biosci. Eng. **12**, 1173–1187 (2015)
33. Ali, A.; Hussain, M.; Ghaffar, A.; Ali, Z.; Nisar, K.S.; Alharthi, M.R.; Jamshed, W.: Numerical simulations and analysis for mathematical model of avascular tumor growth using Gompertz growth rate function. Alexandria Eng. J. **60**, 3731–3740 (2021)
34. Rihan, F.A.; Rahman, D.H.A.: Delay differential model for tumour–immune dynamics with HIV infection of $CD4^+$ T-cells. Int. J. Comput. Math. **90**, 594–614 (2013)
35. Jaroudi, R.; Åström, F.; Johansson, B.T.; Baravdish, G.: Numerical simulations in 3-dimensions of reaction–diffusion models for brain tumour growth. Int. J. Comput. Math. **97**, 1151–1169 (2020)
36. Laib, H.; Bellour, A.; Boulmerka., A.: Taylor collocation method for a system of nonlinear Volterra delay integro-differential equations with application to COVID19 epidemic. Int. J. Comput. Math. **99**(4), 852–876 (2021)
37. He, B.; Meng, Q.: Lump and interaction solutions for a generalized (3 + 1)-dimensional propagation model of nonlinear waves in fluid dynamics. Int. J. Comput. Math. **98**, 592–607 (2021)
38. Li, C.; Yuan, Y.; Yang, Q.: Characteristic mixed volume element for compressible two-phase displacement in porous media. Int. J. Comput. Math. **98**(11), 2233–2250 (2021)
39. Lee, H.-C.; Lee, H.: An adaptive least-squares finite element method for Giesekus viscoelastic flow problems. Int. J. Comput. Math. **98**, 1974–1990 (2021)
40. Jiwari, R.; Gupta, K.; Kumar, V.: Polynomial differential quadrature method for numerical solutions of the generalized Fitzhugh-Nagumo equation with time-dependent coefficients. Ain Shams Eng. J. **5**, 1343–1350 (2014)
41. Salah, M.; Amer, R.M.; Matbuly, M.S.: Analysis of Reaction diffusion problems using differential quadrature method. Int. J. Eng. Technol. **13**, 1–6 (2013)
42. Salah, M.; Amer, R.M.; Matbuly, M.S.: An efficient method to solve thermal wave equations. Appl. Math. **5**, 542–552 (2014)
43. Salah, M.; Amer, R.M.; Matbuly, M.S.: The differential quadrature solution of reaction-diffusion equation using explicit and implicit numerical schemes. Appl. Math. **5**, 327–336 (2014)
44. Dockery, J.D.: Numerical solution of travelling waves for reaction-Diffusion equations via the Sinc–Galerkin method. In: Bowers, K.; Lund J. (eds.) Computation and Control: Proceedings of the Bozeman Conference, pp. 95–113. Montana, United States, (1993).

45. El-Gamel M.; Zayed, A.: A comparison between the wavelet Galerkin and the sincGalerkin methods in solving non homogeneous heat equations. In: Zuhair, N.; Otmar, S. (eds.) Inverse Problems, Image Analysis, and Medical Imaging, American Mathematical Society, Providence, United States, **313** (2002)
46. Yin, G.: Sinc-collocation method with orthogonalization for singular problem-like poisson. Math. Comput. **62**, 21–40 (1994)
47. Carlson, T.S.; Dockery, J.; Lund, J.: A sinc-collocation method for initial value problems. Math. Comput. **66**, 215–235 (1997)
48. Ng, C.H.W.; Zhao, Y.B.; Wei, G.W.: Comparison of discrete singular convolution and generalized differential quadrature for the vibration analysis of rectangular plates. Comput. Methods Appl. Mech. Eng. **193**, 2483–2506 (2004)
49. Wei, G.W.: Discrete singular convolution for the Fokker-Planck equation. Chem. Phys. **110**, 8930–8942 (1999)
50. Wei, G.W.: A unified method for solving Maxwell's equation. Preceding of Asia Pacific Microwave Conference, Institute of Electrical and Electronics Engineers, Singapore **2**, 562–565 (1999)
51. Wei, G.W.: Solving quantum eigenvalue problems by discrete singular convolution. J. Phys. B At. Mol. Opt. Phys. **33**, 343–352 (2000)
52. Wei, G.W.: A unified approach for solving the Fokker-Planck equation. J. Phys. A Math. General **33**, 4935–4953 (2000)
53. Wei, G.W.; Zhao, Y.B.; Xiang, Y.: A novel approach for the analysis of high frequency vibrations. J. Sound Vib. **257**, 207–246 (2002)
54. Wei, G.W.: A new approach for solving some mechanical problems. Comput. Methods Appl. Mech. Eng. **190**, 2017–2030 (2001)
55. Wan, D.C.; Wei, G.W.: Discrete singular convolution-finite subdomain method for the solution of incompressible viscous flows. J. Comput. Phys. **180**, 229–255 (2002)
56. Wei, G.W.; Zhao, Y.B.; Xiang, Y.: The determination of natural frequencies of rectangular plates with mixed boundary conditions by discrete singular convolution. Int. J. Mech. Sci. **43**, 1731–1746 (2001)
57. Wei, G.W.: Discrete singular convolution for the solution of the Fokker-Planck equations. J. Chem. Phys. **110**, 8930–8942 (1999)
58. Shu, C.: Differential quadrature and its application in engineering. Springer, London (2000)
59. Nourazar, S.S.; Soori, M.; Nazari-Golshan, A.: On the exact solution of Newell–Whitehead–Segel equation using the homotopy perturbation method. Aust. J. Basic Appl. Sci. **5**, 1400–1411 (2011)
60. Roy, A. M.: Evolution of Martensitic Nanostructure in NiAl Alloys: Tip Splitting and Bending. Mat. Sci. Res. India; Special Issue (2020). ISSN: 0973–3469, **17**, (Special Issue) 03–06
61. Roy, A.M.: Finite Element Framework for Efficient Design of Three Dimensional Multicomponent Composite Helicopter Rotor Blade System. Eng. **2**, 69–79 (2021). https://doi.org/10.3390/eng2010006

Springer Nature or its licensor (e.g. a society or other partner) holds exclusive rights to this article under a publishing agreement with the author(s) or other rightsholder(s); author self-archiving of the accepted manuscript version of this article is solely governed by the terms of such publishing agreement and applicable law.